

Cdc1 and the Vacuole Coordinately Regulate Mn²⁺ Homeostasis in the Yeast *Saccharomyces cerevisiae*

Madan Paidhungat^{*,1} and Stephen Garrett[†]

^{*}Department of Pharmacology and Cancer Biology, Duke University Medical Center, Durham, North Carolina 27710 and [†]Department of Microbiology and Molecular Genetics, UMDNJ-New Jersey Medical School, University Heights, Newark, New Jersey 07103-2714

Manuscript received August 14, 1997

Accepted for publication December 3, 1997

ABSTRACT

The yeast *CDC1* gene encodes an essential protein that has been implicated in the regulation of cytosolic [Mn²⁺]. To identify factors that impinge upon Cdc1 or the Cdc1-dependent process, we isolated second-site suppressors of the conditional *cdc1-1*(Ts) growth defect. Recessive suppressors define 15 *COS* (*CdcOne Suppressor*) genes. Seven of the fifteen *COS* genes are required for biogenesis of the vacuole, an organelle known to sequester intracellular Mn²⁺. An eighth gene, *COS16*, encodes a vacuolar membrane protein that seems to be involved in Mn²⁺ homeostasis. These results suggest mutations that block vacuolar Mn²⁺ sequestration compensate for defects in Cdc1 function. Interestingly, Cdc1 is dispensable in a *cos16*Δ deletion strain, and a *cdc1*Δ *cos16*Δ double mutant exhibits robust growth on medium supplemented with Mn²⁺. Thus, the single, essential function of Cdc1 is to regulate intracellular, probably cytosolic, Mn²⁺.

CELLS of the yeast *Saccharomyces cerevisiae* divide by budding. Bud development is a complex process that appears to require the metal ion Mn²⁺. Early studies with ion chelators and Ca²⁺ ionophores (Iida *et al.* 1990) suggested that Ca²⁺ was essential for cell growth and proliferation, but a subsequent report suggested Mn²⁺, not Ca²⁺, was the limiting ion (Youat and McKinnon 1993). Yeast cells depleted of both Mn²⁺ and Ca²⁺ exhibit a defect in bud growth, and Mn²⁺ is 500–1000-fold more effective than Ca²⁺ in reversing the growth defect, suggesting that Mn²⁺ is the physiologically important ion (Loukin and Kung 1995).

Yeast Mn²⁺ is present in several subcellular compartments, any one of which might represent, or influence, the Mn²⁺ pool essential for bud growth. The cytosol contains Mn²⁺ as well as such Mn²⁺-dependent enzymes as pyruvate carboxylase, glutamine synthetase, and arginase (Wedler 1994). Mn²⁺ is also present in the Golgi, where it activates glycosyltransferases that are involved in the processing of secreted proteins (Wedler 1994). Mitochondrial Mn²⁺ is required by enzymes of the citric acid cycle (Wedler 1994) as well as proteases involved in mitochondrial protein import (Supek *et al.* 1996). Finally, Mn²⁺ is found in the yeast vacuole (Okorokov *et al.* 1977), an acidic, membrane-bound organelle that has been implicated in Mn²⁺ detoxification. Of these known Mn²⁺-dependent enzymes and processes, only

glycosylation has been shown to affect bud growth. Mutants of *och1*Δ lack a Mn²⁺-dependent Golgi glycosyltransferase and exhibit a conditional defect in bud growth, but Och1 is not essential under standard growth conditions (Nagasu *et al.* 1992). Thus, it is not clear if Och1, or even Golgi Mn²⁺, is related to the Mn²⁺ requirement identified by the depletion studies.

Several proteins have been implicated in intracellular Mn²⁺ homeostasis. Mn²⁺ uptake across the plasma membrane appears to be mediated by Smf1, an integral plasma membrane protein (Supek *et al.* 1996). A second protein, Smf2, shares significant homology with Smf1 and might also be involved in Mn²⁺ uptake (Eide and Gueriot 1997). Of the intracellular organelles, only the Golgi has been characterized in any detail with respect to Mn²⁺ flux. Two structurally unrelated proteins, Pmr1 (a Ca²⁺-ATPase homologue) and Ccc1, seem to play a role in the transport of Mn²⁺ from the cytosol into the Golgi (Lapinskas *et al.* 1995; Lapinskas *et al.* 1996). A third protein, Atx2, has been implicated in the release of Golgi Mn²⁺ into the cytosol (Lin and Culotta 1996). Although two of these proteins (Pmr1 and Smf1) are essential for growth under Mn²⁺-limiting conditions, the phenotypes of Mn²⁺-depleted *pmr1* or *smf1* strains have not been reported. Thus, it is not clear if the activity of either protein affects the Mn²⁺ pool that is required for bud growth.

One factor that does affect the growth-related Mn²⁺ pool is the essential gene *CDC1*. Conditional *cdc1*(Ts) mutants were originally identified on the basis of a defect in bud growth (Hartwell *et al.* 1970), and several lines of evidence implicate Cdc1 in the regulation of cytosolic Mn²⁺. First, Mn²⁺ supplement partially suppresses the *cdc1*(Ts) growth defect (Loukin and Kung

Corresponding author: Stephen Garrett, Department of Microbiology and Molecular Genetics, UMDNJ-New Jersey Medical Center, 185 South Orange Ave., University Heights, Newark, NJ 07103-2714. E-mail: garretst@umdnj.edu

¹Present address: Department of Biochemistry, University of Connecticut Health Center, Farmington, CT 06030.

1995; Paidhungat and Garrett 1998), suggesting that Mn^{2+} is limiting in *cdc1* mutants. Second, defects in *CDC1* cause cells to become sensitive to depletion of cytosolic Mn^{2+} (Supek *et al.* 1996; Paidhungat and Garrett 1998). Finally, *CDC1* overexpression makes certain chelator-sensitive mutants more tolerant to Mn^{2+} depletion (Paidhungat and Garrett 1998). Thus, we propose that the bud-growth defect of *cdc1*(Ts) mutants results from depletion of cytosolic Mn^{2+} , which implies, in turn, that cytosolic Mn^{2+} is critical for bud growth (Paidhungat and Garrett 1998). However, neither the mechanism by which Cdc1 regulates cytosolic Mn^{2+} nor the Mn^{2+} -dependent processes are known.

To identify cellular components that affect the essential Cdc1 function, we isolated suppressors of the *cdc1-1*(Ts) temperature-sensitive growth defect. Several recessive suppressors define genes previously implicated in biogenesis of the vacuole, an organelle known to sequester divalent cations such as Mn^{2+} . In addition, one suppressor gene, *COS16*, encodes a vacuolar membrane protein that appears to be involved in vacuolar Mn^{2+} sequestration. These results suggest mutations that either directly or indirectly block vacuolar Mn^{2+} sequestration compensate for defects in Cdc1 function. Our results also show that Cdc1 is dispensable in cells lacking Cos16, suggesting that Cdc1 function is not required in cells that exhibit a defect in vacuolar Mn^{2+} sequestration. Thus, it seems likely that the essential function of Cdc1 is to maintain cytosolic $[Mn^{2+}]$ above a minimum threshold that is required for growth.

MATERIALS AND METHODS

Media: Standard yeast media were prepared as previously described (Paidhungat and Garrett 1998). LiCl and $MgCl_2$ were added to rich yeast medium (YEPD) after autoclaving. Medium containing $CaCl_2$ was made by autoclaving YEPD medium, buffering to pH 5.5 with 50 mM succinate/NaOH and then adding $CaCl_2$ to the indicated concentration.

Strains and plasmids: Revertants were derived from strains FY11 [*MAT α ade1 trp1 leu2 his3 ura3 cdc1-1*(Ts)] and FY12 [*MAT α ade8 trp1 leu2 his3 ura3 cdc1-1*(Ts)]. Strain FY70 (FY11 *CDC1*) was derived from FY11 by reversion and contains the wild-type *CDC1* allele. Strain FY71 (*MAT α ade8 trp1 leu2 his3 ura3 CDC1*) has been described (Paidhungat and Garrett 1998) and was used to determine suppressor linkage to *CDC1*. Diploid strain FY1 (*MAT α /MAT α cdc1 Δ ::*HIS3/CDC1 ade2/ADE2 trp1/TRP1 ura3/ura3 leu2/leu2 his3/his3 lys2/lys2*) and a *cos16* Δ derivative (FY1 *cos16 Δ ::LEU2/COS16*) were derived from strain Y1029 (Garrett and Broach 1989) by transformation. Bacterial strains MC1066 and DH5 α were used for plasmid manipulations and have been described (Casadaban *et al.* 1983; Woodcock *et al.* 1989).*

Plasmid YEp13-*CDC1* (pFB28) has been described (Paidhungat and Garrett 1998). Plasmid YIp5-*CDC1* (pFB56) was constructed by inserting the 3.5-kb *HindIII CDC1* fragment into the *HindIII* site of YIp5 (NEB catalogue; New England Biolabs, Beverly, MA). The resulting plasmid was integrated at the *CDC1* locus by linearizing with *XbaI* before yeast transformation.

Genetic manipulations: The *cdc1*(Ts) revertants were iso-

lated by patching independent colonies of FY11 and FY12 onto YEPD agar plates, which were then incubated at either 30° or 36° for 2 days. Temperature-resistant revertants arose as papillae from the patches; a single papilla was picked from each patch to ensure that revertants were independent. At 23°, two revertants gave rise to small, temperature-resistant colonies as well as large, temperature-sensitive colonies. Crosses showed that the small colonies were disomic for chromosome IV, whereas the large colonies contained a single copy of chromosome IV.

Cloning *COS4*, *COS5*, and *COS15*: *COS4*, *COS5*, and *COS15* were cloned from a YCp50-based yeast genomic library (Rose *et al.* 1987) by their ability to complement the temperature-sensitive growth defects of *cos4-8 cdc1-1* [YEp13-*CDC1*], *cos5-17 cdc1-1* [YEp13-*CDC1*], and *cos15-118 cdc1-1* [YEp13-*CDC1*] strains, respectively. Four *COS4* plasmids, pFB77–pFB80, contained distinct, but overlapping, genomic regions that also reversed the temperature-resistant growth of a *cos4-8 cdc1-1*(Ts) strain. Plasmid pFB87 was generated by subcloning the 4.3-kb *HindIII-BglII* genomic fragment from pFB78 into the *HindIII* and *BamHI* sites of the low-copy *URA3* vector pRS316 (Sikorski and Hieter 1989). This fragment complemented all of the *cos4* mutant phenotypes and was physically linked to the *PEP3* region (Riles *et al.* 1993). The *PEP3* gene was disrupted by inserting the *HIS3* marker into a unique *BamHI* site in pFB78 to generate plasmid pFB107. The *pep3::HIS3* disruption was excised from pFB107 using *EcoRI*.

Seven (pFB94–pFB100) of eleven *COS5* plasmids recovered contained distinct, but overlapping, genomic regions. Plasmid pFB109 was constructed by inserting the 4.6-kb *BglII-BamHI* fragment from pFB99 into the *BamHI* site of pRS316. This plasmid complemented all of the *cos5* mutant phenotypes. Plasmid pFB162 was used to mark the *COS5* locus and was constructed by inserting the 1.9-kb *EcoRI* fragment from pFB109 into a derivative (pFB119) of the integrating vector pRS306, which lacked the *SpeI* and *XbaI* sites in the multiple cloning sequence (MCS). Plasmid pFB162 was linearized at the unique *XbaI* site in the insert and integrated by homology-directed recombination into the yeast genome.

Two identical *COS15* plasmids, pFB135 and pFB136, contained the *PEP5* gene, as determined by comparing its restriction map to that of a YCp50-*PEP5* plasmid obtained from E. Jones (Carnegie Mellon University, Pittsburgh).

Cloning and disruption of *COS8*: The *COS8* gene was originally cloned as a high-copy suppressor of the *cdc1-1*(Ts) growth defect. Plasmid pFB57 was isolated from a high-copy (pRS202) yeast genomic library (C. Connelly and P. Hieter, unpublished results) by its ability to suppress the temperature-sensitive growth defect of strain FY11 (*cdc1-1*) at 30°. A 1.8-kb *HindIII* genomic fragment from pFB57 was subcloned into the *HindIII* site of pRS202 to generate plasmid pFB67, which suppressed the *cdc1-1*(Ts) temperature-sensitive growth defect. Interestingly, plasmid pFB67 complemented the salt sensitivity of the *cos8* mutants. To determine if pFB57 contained *COS8*, the 1.8-kb *HindIII* fragment was subcloned into the low-copy vector pRS316. The resulting plasmid, pFB161, complemented all of the *cos8* mutant phenotypes. The 1.8-kb *HindIII* fragment was physically mapped to a region of chromosome XVI (Riles *et al.* 1993 and references therein) that contained a single, complete open reading frame, *VPS4/END13*.

The 1.8-kb *HindIII COS8* fragment was inserted into pUC8 (NEB catalogue) to generate plasmid pFB217. Two different derivatives of pFB217 were used to disrupt the chromosomal *COS8* gene. In the first construct, the *URA3* marker was inserted into a unique *MscI* site in *COS8* to generate plasmid pFB277. The *cos8::URA3* disruption was liberated from plasmid pFB277 with *KpnI*, and transplanted into the yeast genome. To

confirm the *cos8::URA3* disruption from pFB277 represented the complete loss of Cos8 function, a *cos8Δ::URA3* deletion was constructed from pFB217 by replacing the *EcoRV-SpeI* region of *COS8* with *URA3* to generate plasmid pFB275. The *cos8Δ::URA3* disruption was liberated with *HindIII* and transplanted into the yeast genome. Although transformation frequencies using the second construct were reduced by the limited flanking homology, transformants derived from either construct exhibited identical phenotypes.

Cloning *COS9*: The recessive, cold-sensitive (18°) growth defect of the *cos9-26*(Cs) revertant was exploited to select *COS9* clones from a low-copy yeast genomic library (Rose *et al.* 1987). Two plasmids, pFB188 and pFB190, containing overlapping regions complemented the conditional growth defect of the *cos9-26*(Cs) strain and reversed the temperature-resistant growth of a *cdc1-1*(Ts) *cos9-26*(Cs) double mutant at 30°. A 1.0-kb *EcoRI-XbaI* complementing fragment from plasmid pFB188 was subcloned into pRS316 to generate plasmid pFB220. This region was physically linked to the *ARF1* region on chromosome *IVL* (Riles *et al.* 1993 and references therein). A frameshift mutation was introduced into the *ARF1* gene by digesting pFB220 with *BglII* and filling in the staggered ends to generate plasmid pFB254. The *arf1Δ::HIS3* construct was obtained from Dr. R. Kahn (Emory University, Atlanta).

Cloning *COS16*: The *COS16* gene was cloned from a low-copy yeast genomic library (Rose *et al.* 1987) by screening for temperature-sensitive transformants of a *cdc1-1*(Ts) *cos16-57* mutant. Two plasmids (pFB163 and pFB164) with overlapping inserts were recovered. Plasmids pFB168 and pFB169 were derived from the low-copy *LEU2* vector pRS315 (Sikorski and Hieter 1989) and contained 2.7-kb *PstI-BamHI* and 3.2-kb *HindIII-PstI* fragments, respectively, from pFB163. Plasmid pFB179 was generated by inserting a complementing 2.1-kb *BglIII-SpeI* (the *SpeI* site was from the MCS) fragment from pFB168 between the *BamHI* and *XbaI* sites of pRS316. Physical analysis of the 2.1-kb fragment (Riles *et al.* 1993 and references therein) showed it contained a single, complete open reading frame, *YCR44c*. A frameshift mutation was introduced into *YCR44c* by linearizing pFB179 at the unique *XbaI* site within *YCR44c*, filling in the staggered ends, and religating to generate plasmid pFB182.

The *cos16Δ::HIS3* disruption was generated in several steps. First, the 2.7-kb *PstI-BamHI* insert from pFB168 was inserted into the *XbaI* and *XhoI* sites of pRS306, using the *SpeI* and *SalI* sites of the pFB168 MCS. This left unique *XhoI* and *XbaI* sites in the insert of the resulting plasmid pFB211. The 0.6-kb *XhoI-XbaI* fragment within the *COS16* coding region of pFB211 was replaced with a *XhoI-XbaI HIS3* fragment to generate plasmid pFB218. The *cos16Δ::HIS3* allele was transplanted into the yeast genome after liberating it from plasmid pFB218 with *EcoRI*. The *cos16Δ::LEU2* allele was constructed by replacing the *XhoI-SnaBI* region of *YCR44c* in plasmid pFB211 with a *SalI-HpaI LEU2* fragment to generate plasmid pFB371. The *cos16Δ::LEU2* allele was liberated from pFB371 with *BamHI* and *BglII*.

The *COS16-lacZ* fusion was generated by inserting the *MifI* fragment carrying the *COS16* open reading frame into the *EcoRI* site of YEp356R (Myers *et al.* 1986) to generate plasmid pFB325. This fusion lacked the carboxy-terminal residue of the Cos16 protein. An integrating version (pFB333) of the *COS16-lacZ* fusion plasmid was constructed by inserting the *AatII COS16-lacZ* fusion fragment from pFB325 in place of the homologous *AatII* fragment of Yp356R (Myers *et al.* 1986). Plasmid pFB333 was integrated at the *URA3* locus after linearizing with *StuI*.

Vacuolar staining and carboxypeptidase Y (CPY) secretion: Log-phase cells were stained with the vital vacuolar dye CDCFDA (Molecular Probes, Eugene, OR), using a procedure described previously (Manolson *et al.* 1992), except that

CDCFDA was used instead of CFDA. CPY secretion was detected by a colony hybridization assay (Roberts *et al.* 1991).

Isolation of vacuoles and Cos16 localization: Crude fractionation of cell extracts was performed as described (Cowles *et al.* 1994), except that the ³⁵S-labeling step was omitted. Vacuoles were purified as described (Cardenas *et al.* 1995; Ohsumi and Anraku 1981), with the exception that the SW40Ti rotor was used for ultracentrifugation (rpms were adjusted to generate the required *g* force). Protein content of extracts was measured by the Bradford assay (Bio-Rad, Richmond, CA) with BSA standards. For antigen detection and quantitation, extracts were diluted into sample buffer, heated at 65° for 10 min, separated on 10% SDS-PAGE, and blotted to nitrocellulose (Shleicher and Schuell, Keene, NH). The Cos16-LacZ fusion protein was detected with α-β-Gal antiserum (Cappel Research Products). CPY and Vph1 were detected with monoclonal antibodies from Molecular Probes (Eugene, OR). Kar2 and Pma1 were detected using antisera obtained from M. D. Rose (Princeton University, Princeton, NJ) and M. Cardenas (Duke University Medical Center, Durham, NC), respectively. HRP-conjugated secondary antibodies (Sigma Chemical, St. Louis; Promega, Madison, WI) were used for detection with the ECL system (Amersham, Arlington Heights, IL).

Mn²⁺ estimation: The cells were prepared as previously described (Lapinskas *et al.* 1995), and concentrated by centrifugation to 20–80 A₆₀₀ units/ml. The cell slurry (25 μl, 1–2 A₆₀₀ units) was digested with 50% nitric acid for 2 hr at 95° (until solution cleared) in an acid-rinsed Eppendorf tube, cooled to room temperature, and diluted to 1 ml with deionized water. Atomic absorption spectroscopy was performed with a L'vov platform furnace in a Z3030 (Perkin-Elmer, Norwalk, CT) instrument with 25 μg Mg(NO₃)₂ (Sigma Chemical, ACS grade) matrix modifier. The furnace temperature program was: Dry 140° (10 sec ramp, 60 sec hold); Char 1400° (8 sec ramp, 25 sec hold); Atomize and reading 2200° (0 sec ramp, 5 sec hold); Clean 2650° (1 sec ramp, 4 sec hold); Cool 20° (1 sec ramp, 30 sec hold). Argon gas flow was maintained at 300 ml/min, except during atomization (0 ml/min). Each digested sample was analyzed twice and averaged. The results of two independent experiments are shown. The Mn²⁺ content in each sample was normalized to the A₆₀₀.

RESULTS

Suppressors of the *cdc1-1*(Ts) temperature-sensitive growth defect: Suppressors of the *cdc1-1*(Ts) growth defect were isolated by selecting spontaneous, temperature-resistant revertants of *MATα cdc1-1*(Ts) and *MATα cdc1-1*(Ts) strains (see materials and methods). Fifty-four independent revertants were isolated at 30°, and two revertants were recovered at 36°. None of the revertants isolated at 30° grew at 36°, suggesting that the growth defect at 30° was less severe than that at 36° (Figure 1). Three of the 54 revertants isolated at 30°, and both revertants isolated at 36°, contained dominant suppressors. Temperature-resistant growth segregated 2:2 in all cases, indicating that each revertant carried a single nuclear suppressor mutation.

Intragenic suppressors were identified by crossing each *cdc1-1*(Ts) *cos* (*cdc16* suppressor) strain to a wild-type *CDC1 COS* strain, and examining tetrads for temperature-sensitive recombinants [*cdc1-1*(Ts) *COS*]. Suppressors in both revertants isolated at 36°, as well as one

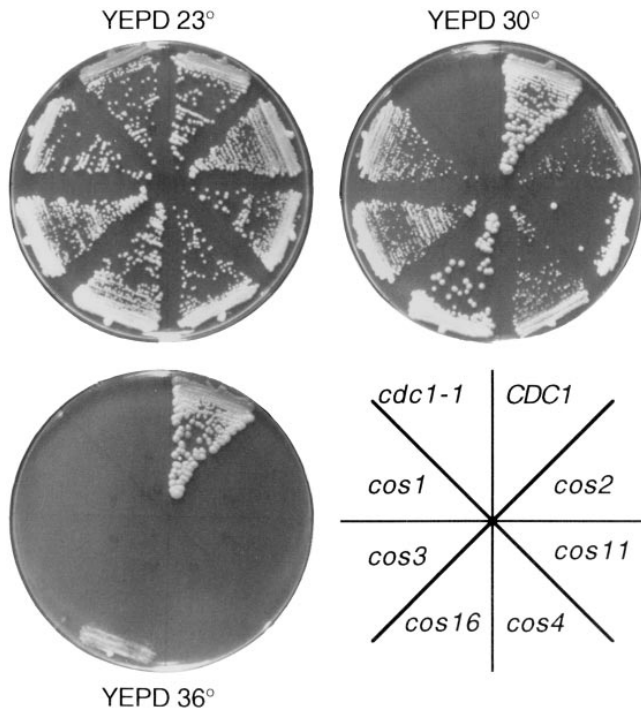


Figure 1.—Suppressors of the *cdc1-1(Ts)* growth defect. The parent *cdc1-1(Ts)* strain and seven spontaneous revertants were streaked onto YEPD agar and incubated at 23°, 30°, and 36°. Strains were: *CDC1* (FY70 = FY11 *CDC1*); *cos2* (FY11 *cos2-2*); *cos11* (FY11 *cos11-29*); *cos4* (FY11 *cos4-8*); *cos16* (FY11 *cos16-57*); *cos3* (FY11 *cos3-3*); *cos1* (FY11 *cos1-1*); *cdc1-1* (FY11).

recessive revertant isolated at 30°, failed to recombine with the *cdc1-1(Ts)* lesion (>30 tetrads examined). The *cdc1-1(Ts)* allele resulted from a single C to T transition [Pro₃₅₁ (CCT) to Leu₃₅₁ (CTT)]. The *CDC1* gene from one of the revertants (FY70) isolated at 36° contained the wild-type CCT sequence at codon 351; the recessive intragenic suppressor, *cdc1-130*, retained the original *cdc1-1(Ts)* lesion and a second C to T transition [Thr₂₃₁ (ACA) to Ile₂₃₁ (ATA)].

Aberrant segregation of the *ade8* marker suggested two recessive revertants were disomic for chromosome IV. Because *CDC1* is located on chromosome IV, it seemed likely that *cdc1-1(Ts)* duplication was sufficient to allow growth at 30°. Consistent with this idea, a *cdc1-1(Ts)* haploid strain carrying an extra copy of the *cdc1-1(Ts)* allele on an integrating plasmid grew at 30° (data not shown). By contrast, a diploid strain containing four copies of the *cdc1-1(Ts)* allele failed to grow at 30° (data not shown). Thus, diploid cells need disproportionately more Cdc1 activity than haploid cells. This may explain why one of the intragenic suppressors (*cdc1-130*) and the chromosome IV duplications were recessive.

Recessive suppressors define 15 genes that fall into four phenotypic groups: Forty-eight of the 54 suppressors isolated at 30° were recessive, and unlinked to *CDC1*. These were placed into complementation groups by testing diploids from pairwise matings of the *cdc1(Ts)*

TABLE 1
Recessive suppressors of *cdc1-1(Ts)* define 15 complementation groups

Locus	Mutant allele(s) recovered
<i>cos1</i>	<i>cos1-1</i> , <i>cos1-124</i>
<i>cos2</i>	<i>cos2-2</i> , <i>cos2-6</i> , <i>cos2-13</i> , <i>cos2-16</i> , <i>cos2-19</i> , <i>cos2-22</i> , <i>cos2-27</i>
<i>cos3</i>	<i>cos3-3</i> , <i>cos3-109</i> , <i>cos3-115</i> , <i>cos3-127</i> , <i>cos3-129</i>
<i>pep3</i> (<i>cos4</i>)	<i>pep3-8</i> , <i>pep3-112</i> , <i>pep3-122</i>
<i>vph4</i> (<i>cos5</i>)	<i>vph4-17</i>
<i>cos6</i>	<i>cos6-18</i>
<i>cos7</i>	<i>cos7-20</i> , <i>cos7-31</i>
<i>vps4</i> (<i>cos8</i>)	<i>vps4-21</i> , <i>vps4-23</i> , <i>vps4-130</i>
<i>arf1</i> (<i>cos9</i>)	<i>arf1-26</i> (Cs), <i>arf1-32</i> , <i>arf1-132</i>
<i>cos10</i>	<i>cos10-28</i>
<i>cos11</i>	<i>cos11-29</i> , <i>cos11-113</i>
<i>cos13</i>	<i>cos13-101</i> , <i>cos13-125</i>
<i>cos14</i>	<i>cos14-102</i> , <i>cos14-103</i> , <i>cos14-116</i> , <i>cos14-120</i> , <i>cos14-131</i> <i>pep5</i> (<i>cos15</i>) <i>pep5-118</i>
<i>cos16</i>	<i>cos16-57</i> , <i>cos16-128</i>

cos isolates for growth at 30°. By this analysis, 40 of the 48 suppressors were assigned to 15 different complementation groups (Table 1).

Several *cdc1-1(Ts)* *cos* double mutants were sensitive to salts at 23°. To examine the salt sensitivity in more detail, we transformed a representative mutant from each complementation group with a Ylp5-*CDC1* plasmid, and tested growth on medium containing 200 mM CaCl₂, 200 mM MgCl₂, and 100 mM LiCl. Seven *CDC1 cos* mutants (*cos4*, *cos5*, *cos15*, *cos6*, *cos11*, *cos8*, and *cos9*) exhibited varying degrees of sensitivity to all of the salts tested (Figure 2 and data not shown; *cos6* and *cos11* mutants were less sensitive than *cos4* mutants to all salts, and their sensitivity to 200 mM MgCl₂ is not readily apparent in the figure). Interestingly, three *cos* mutants (*cos1*, *cos3*, and *cos14*) were sensitive only to CaCl₂ and LiCl, two *cos* mutants (*cos13* and *cos16*) were specifically sensitive to MgCl₂ (Figure 2 and data not shown), and three *cos* mutants (*cos2*, *cos7*, and *cos10*) did not exhibit measurable sensitivity to any of the salts tested (Figure 2 and data not shown). In all cases, salt sensitivity and *cdc1-1(Ts)* suppression were tightly linked (no recombination in >10 tetrads), implying a single mutation was responsible for both phenotypes. Finally, sensitivity to specific cations probably reflects differences in the cellular functions of particular *COS* genes because all of the mutants within each of the latter complementation groups (*cos1*, *cos3*, *cos14*, *cos13*, *cos16*, *cos2*, *cos7*, and *cos10*) exhibited sensitivity to the same range of cations as the representative isolate (Figure 2 and data not shown). Accordingly, the *CDC1 cos* mutants were divided into four broad phenotypic groups, I to IV (Table 2). Mutations in three group III genes, *COS4*, *COS5*, and

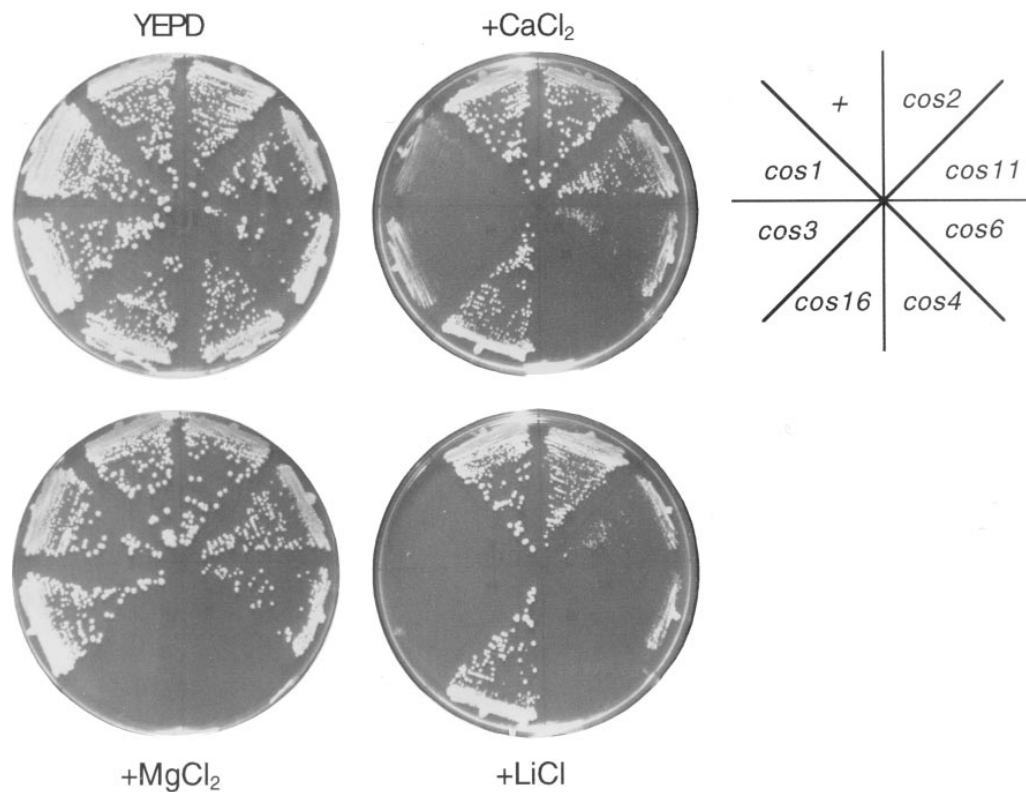


Figure 2.—Salt tolerance of the *cos* mutants. The indicated strains were transformed with the YIp5-*CDC1* plasmid, and then streaked onto YEPD agar, YEPD pH 5.5 agar containing 200 mM CaCl₂, YEPD agar containing 200 mM MgCl₂, or YEPD agar containing 100 mM LiCl, and incubated at 30° for 3–5 days. Strains were: *cos2* (FY11 *cos2-2*); *cos11* (FY11 *cos11-29*); *cos6* (FY11 *cos6-18*); *cos4* (FY11 *cos4-8*); *cos16* (FY11 *cos16-57*); *cos3* (FY11 *cos3-3*); *cos1* (FY11 *cos1-1*); + (FY11).

COS15, also blocked accumulation of red pigment in an *ade1* background and conferred a temperature-sensitive (36°) growth defect in a *CDC1* strain (data not shown). Thus, group III genes were subclassified as group IIIA (*COS4*, *COS5*, and *COS15*), and group IIIB (*COS6*, *COS8*, *COS9*, and *COS11*).

Group IIIA *COS* genes are identical to class C *VPS* genes: The *ade1* pigment-accumulation defect, temperature sensitivity, and salt sensitivity of the group IIIA *cos* mutants resembled phenotypes exhibited by a subset of

vacuolar protein sorting (*vps/pep*) mutants (Banta *et al.* 1988). The group IIIA *cos* mutants also displayed several additional phenotypes exhibited by a subset of the *vps/pep* mutants, including sensitivity to 500 mM NaCl, 4 mM ZnCl₂, and 8 mM MnCl₂, as well as failure to sporulate as homozygous diploids (data not shown). To determine if group IIIA *COS* genes were related to known *VPS* genes, we isolated the *COS4*, *COS5*, and *COS15* genes from a yeast genomic library by complementing the temperature-sensitive growth defect of *CDC1 cos4*, *CDC1 cos5*, and *CDC1 cos15* strains, respectively (see materials and methods). We also examined the ability of *cos4*, *cos5*, and *cos15* mutants to complement the phenotypes of known *vps/pep* mutants. These studies showed (Table 1) that *COS4* is identical to *VPS18/PEP3* (Preston *et al.* 1991; Robinson *et al.* 1991), *COS5* is identical to *VPS16/VPH4* (Horazdovsky and Emr 1993; Preston *et al.* 1992), and *COS15* is identical to *VPS11/PEP5* (Woolford *et al.* 1990). Finally, these assignments were confirmed by showing that mutations inactivating *VPS18* (*pep3::LEU2*), *VPS16* (*vph4-5*) or *VPS11* (*pep5Δ::URA3*), as well as a fourth class C *VPS* gene *VPS33* (*pep14-5*) (Banta *et al.* 1990) suppressed the growth defect of a *cdc1-1*(Ts) strain at 30° (data not shown). Thus, mutations in all four class C *VPS* genes suppressed the *cdc1-1*(Ts) growth defect at 30°.

Group IIIB *cos* mutants mislocalize the vacuolar protein CPY: Group IIIB *cos* mutants shared several phenotypes with the class C *vps* mutants, including general salt sensitivity and a sporulation defect, with the class C

TABLE 2

Phenotypic grouping of *COS* genes

Group	Complementation groups/Loci	Sensitivity to: ^a
I	<i>cos</i> , <i>cos3</i> , <i>cos14</i> ^b	CaCl ₂ , LiCl
II	<i>cos13</i> , <i>cos16</i>	MgCl ₂
III	Group IIIA: <i>pep3</i> (<i>cos4</i>), <i>vps16</i> (<i>cos5</i>), <i>pep5</i> (<i>Cos15</i>) Group IIIB: <i>vps4</i> (<i>cos8</i>), <i>cos6</i> , <i>cos11</i> , <i>arf1</i> (<i>cos9</i>)	CaCl ₂ , LiCl, MgCl ₂ , MnCl ₂ , ZnCl ₂ CaCl ₂ , LiCl, MgCl ₂ , MnCl ₂ , ZnCl ₂ ; sensitivity less severe than group IIIA
IV	<i>cos2</i> , <i>cos7</i> , <i>cos10</i>	None

^a Sensitivity to: 200 mM CaCl₂; 200 mM MgCl₂; 100 mM LiCl; 4 mM ZnCl₂; 8 mM MnCl₂.

^b All strains were *CDC1*.

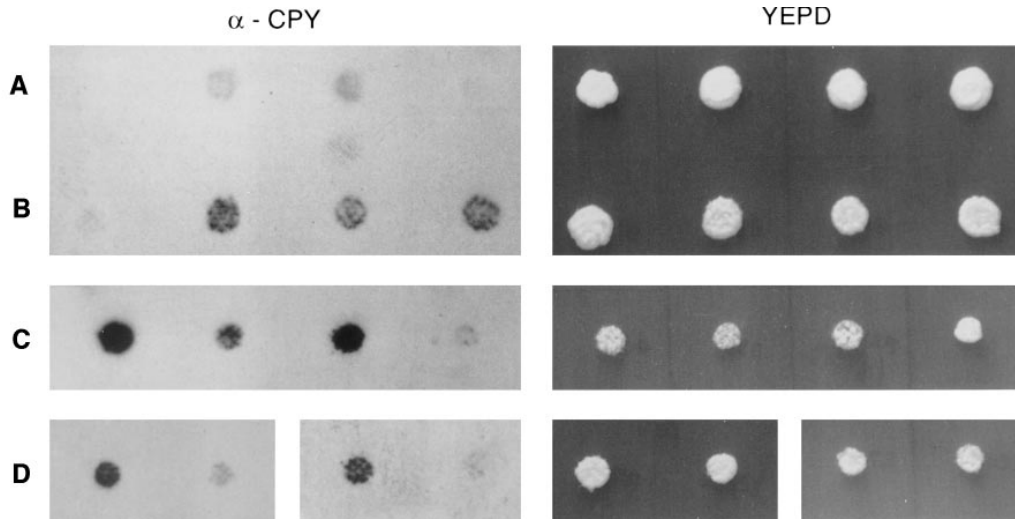


Figure 3.—CPY secretion. Patches of the indicated strains were replica plated to YEPD agar, overlaid with nitrocellulose membrane, and incubated at 23°. After 12 hr, membranes were rinsed in water and probed with α -CPY antibodies. All strains in rows A–C carried a Ylp5-*CDC1* plasmid. Strains were, from left to right, row A: FY11 *cos16-57*, FY11 *cos3-3*, FY11 *cos1-1*, and FY11; row B: FY11 *cos2-13*, FY11 *cos11-29*, FY11 *cos6-18*, and FY11 *pep3-8*; row C: FY11 *arf1-32*, FY11 *pep3-8*, FY11 *vps4-21*, FY11; row D: FY70 [pRS202-*COS4*], FY70 [pRS202], FY11 [pRS202-*COS4*], FY11 [pRS202].

vps mutants (although *cos9* mutants did not exhibit a sporulation defect). To determine if group IIIB *COS* genes were also involved in vacuolar protein sorting, we examined localization of the vacuolar protein CPY. Wild-type strains efficiently target CPY to the vacuole. Mutants with defects in the vacuolar protein sorting pathway, by contrast, secrete significant amounts of CPY (Raymond *et al.* 1992). Similar to the class C *vps18* (*cos4-8*) mutant, all of the group IIIB *cos* mutants (*cos6*, *cos8*, *cos9*, and *cos11* mutants) secreted significantly more CPY than the wild-type strain (Figure 3, B and C). The sorting defect was less apparent, but nevertheless obvious, in the *cos9* mutant (Figure 3C). Thus, group IIIB *COS* genes are necessary for efficient vacuolar protein sorting. By contrast, *cos* mutants from groups II and IV did not exhibit significant CPY secretion (Figure 3), and group I *cos* mutants displayed a slight defect in CPY secretion (Figure 3A) that became more severe in older colonies.

Mutations in class D *VPS* genes suppress the *cdc1-1*(Ts) growth defect: To determine if group IIIB *cos* mutations affected vacuolar biogenesis, we examined vacuolar morphology using the vital stain CDCFDA. In contrast to the multilobed vacuolar structure of wild-type cells (Figure 4), *cos6* and *cos11* mutant cells displayed a single vacuolar lobe (Figure 4 and data not shown) that was similar to the abnormal vacuolar morphology of class D *vps* mutants (Raymond *et al.* 1992). Like class D *vps* mutants, *cos6* and *cos11* cells failed to form vacuolar segregation structures and exhibited a defect in vacuolar inheritance (Figure 4 and data not shown). Finally, disruption of the class D *VPS* gene, *VPS19/PEP7/VAC1* (Weisman and Wickner 1992), alleviated the growth defect of a

cdc1-1(Ts) mutant at 30° (data not shown). Thus, loss of class D Vps function suppressed the *cdc1*(Ts) growth defect. *COS6* and *COS11* were distinct from *PEP7* and might define other class D *VPS* genes.

***COS8* is identical to *VPS4/END13*, a class E *VPS* gene:** *cos8* cells exhibited a single, prominent vacuolar structure surrounded by one or more small, CDCFDA-staining vesicles (Figure 4). Although this vacuolar morphology resembled that of wild-type cells (Figure 4), class A and class E *vps* mutants also contain normal-looking vacuoles (Raymond *et al.* 1992). Indeed, molecular characterization (see materials and methods) showed that *COS8* was identical to *VPS4/END13*, a class E *VPS* gene implicated in vacuolar protein sorting (Munn and Riezman 1994). Furthermore, a *vps4 Δ ::URA3* disruption suppressed the *cdc1-1*(Ts) growth defect at 30° (data not shown), indicating that loss of class E Vps function suppressed the *cdc1-1*(Ts) growth defect.

Because *VPS4* was also identified as a high-copy suppressor of the *cdc1-1*(Ts) growth defect (see materials and methods), we determined if Vps4 overproduction blocked vacuolar protein sorting. As shown in Figure 3D, an increase in *VPS4* dosage caused *CDC1* and *cdc1-1*(Ts) cells to secrete more CPY, consistent with the idea that Vps4 overproduction suppressed the *cdc1-1*(Ts) growth defect by impeding vacuolar protein sorting.

Loss of Arf1 function suppresses the *cdc1-1*(Ts) growth defect: The last group IIIB mutant, *cos9*, displayed numerous (>15) CDCFDA-staining vesicles, indicative of vacuolar fragmentation (Figure 4; this phenotype was clearer under Nomarski optics because vesicles outside the focal plane interfered with visualization of the CDCFDA fluorescence). Interestingly, *cos9* mutants also exhibited abnor-

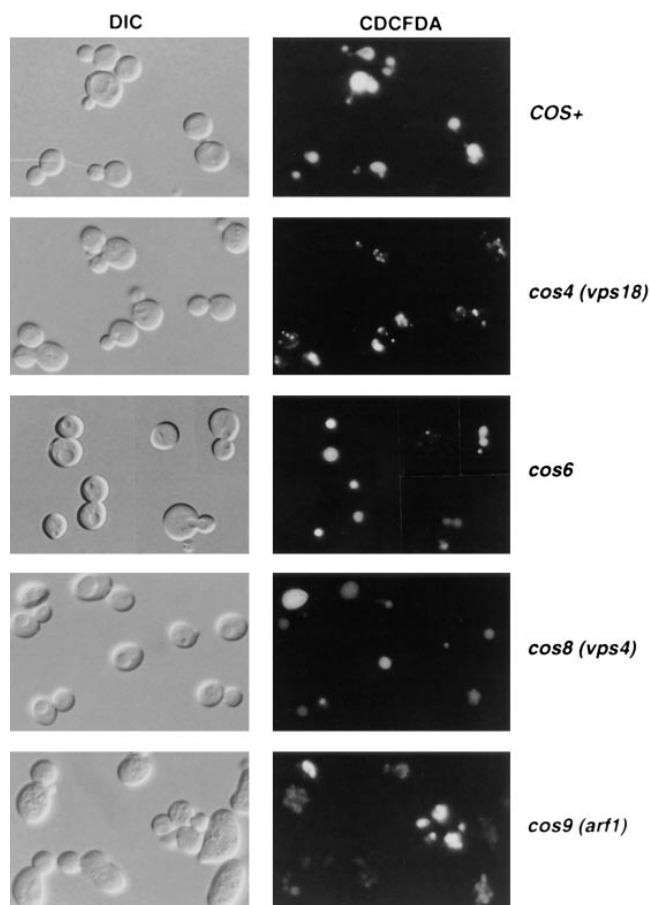


Figure 4.—Vacuolar morphology of *cos* mutants visualized by CDCFDA. Exponentially growing cells were stained with the vital dye CDCFDA and visualized by differential interference contrast (DIC) or fluorescence (CDCFDA) microscopy. Strains: *COS+* (FY11 [YIp5-*CDC1*]); *cos4* (*vps18*) (FY11 *cos4-8* [YIp5-*CDC1*]); *cos6* (FY11 *cos6-18* [YIp5-*CDC1*]); *cos8* (*vps4*) (FY11 *cos8-21* [YIp5-*CDC1*]); *cos9* (*arf1*) (FY11 *cos9-32* [YIp5-*CDC1*]).

morphologies in cell size and shape (Figure 4), suggesting *Cos9* might affect several cellular processes. We cloned *COS9* and found it was identical to the *ARF1* gene (see materials and methods), which encodes a GTPase implicated in transport between the endoplasmic reticulum (ER) and Golgi compartments (Stearns *et al.* 1990). As expected, the *arf1Δ::HIS3* disruption allowed a *cdc1-1*(Ts) mutant to grow at 30° (data not shown). Although *ARF1* has not been previously described as a *VPS* gene, the *arf1Δ::HIS3* mutant secreted CPY, displayed abnormal vacuolar morphology, and exhibited decreased tolerance to salt. Because *Arf1* function is required for normal vacuolar biogenesis, the *cos9* mutations probably suppress the *cdc1-1*(Ts) growth defect by debilitating vacuolar function.

Proteinase A deficiency does not suppress the *cdc1-1*(Ts) growth defect: Because the group III *cos* mutations blocked formation of a normal vacuole, the *cdc1*(Ts) growth defect was probably alleviated by the absence of a normal vacuole, rather than a defect at a specific stage of vacuolar protein sorting. The yeast vacuole plays a

major role in protein turnover. Several vacuolar hydrolases, including proteinase B and CPY, are activated by the vacuolar Pep4 proteinase (proteinase A). As a result, loss of Pep4 function results in a 90–95% reduction in vacuolar hydrolase activity (Jones *et al.* 1982). Nevertheless, a *cdc1-1*(Ts) *pep4Δ::LEU2* strain failed to grow at 30° (data not shown). Thus, neither the loss of Pep4 nor the accompanying reduction in vacuolar hydrolase activity could account for *cdc1*(Ts) suppression by defects in vacuolar biogenesis.

Group II gene *COS16*: The group II *cos* mutants exhibited a subset of the group III *cos* mutant phenotypes, including Mg²⁺ sensitivity (Figure 2), failure to sporulate, and a slight growth defect at 36° (data not shown). However, group II *cos* mutants did not secrete CPY (Figure 3). We cloned the *COS16* gene from a yeast genomic library by complementation of the temperature-resistant growth of the *cdc1-1*(Ts) *cos16-57* mutant. The complementing fragment was mapped to a region of chromosome *IIIR* (data not shown), which contained a single 1071-bp open reading frame, *YCR44c*. A frameshift mutation introduced into the *YCR44c* coding region abolished the ability of the 2.1-kb fragment to complement the *cos16-57* mutation (data not shown). In addition, a *YCR44c* disruption suppressed the *cdc1*(Ts) temperature-sensitive growth defect (data not shown) and conferred Mg²⁺ sensitivity and temperature-sensitive growth (at 36°) to a *CDC1* strain (data not shown). Finally, all of the spontaneous *cos16* alleles were tightly linked (<2.5 cM with at least 20 tetrads) to the *MAT* locus, as predicted by the physical proximity of *YCR44c* to *MAT*. Thus, *COS16* is identical to the open reading frame *YCR44c*.

Subcellular localization of *Cos16*: The predicted primary structure of the *Cos16* protein did not exhibit significant homology to proteins in the available databases. Nevertheless, hydropathy analysis (Kyte and Doolittle 1982) showed that *Cos16* contained 8 putative membrane-spanning helices, suggesting that it was an integral membrane protein. To examine *Cos16* localization, we constructed a hybrid gene between *COS16* and *lacZ*. A single copy of the *COS16-lacZ* fusion was integrated at the *URA3* locus in a *cos16Δ::HIS3* mutant. Most (>80%) of the *Cos16-LacZ* fusion protein was detected in the particulate fraction (100,000 *g* for 1 hr), and could be solubilized with Triton X-100, but not 1 M NaCl or 2 M urea (data not shown). Thus, the *Cos16-LacZ* fusion protein is probably an integral membrane protein.

The subcellular localization of the *Cos16-LacZ* fusion protein was initially examined by crude fractionation. Cell lysates were fractionated by sequential centrifugation (Cowles *et al.* 1994), and the fusion protein in each fraction was detected by Western blotting. Greater than 90% of the *Cos16-LacZ* fusion protein cofractionated with the vacuolar membrane marker, *Vph1*, as well as the ER luminal marker, *Kar2*, in the P13 fraction (data not shown). To determine if *COS16* encoded a vacuolar membrane protein, vacuoles were purified by

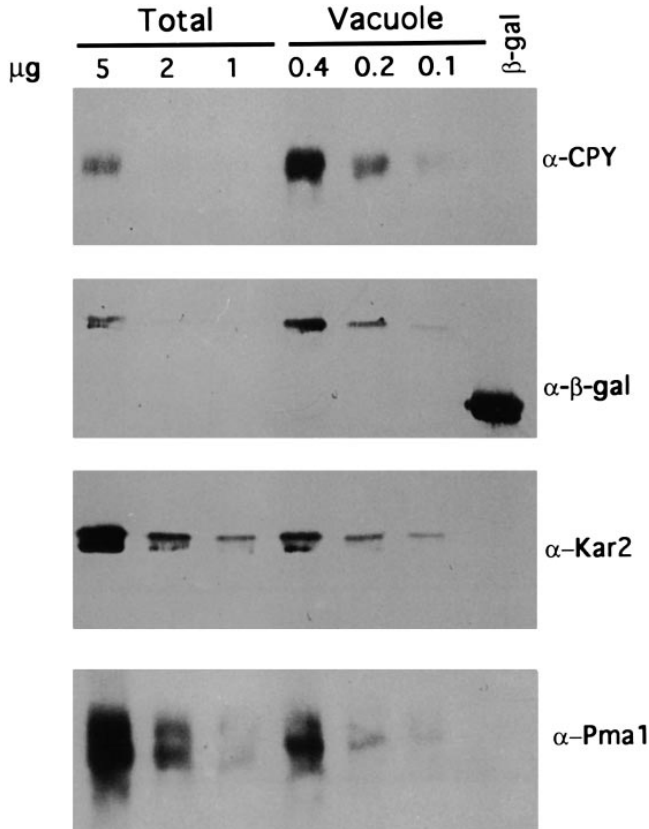


Figure 5.—Subcellular localization of Cos16- β -gal fusion protein. Protein from whole-cell lysates (Total) or purified vacuoles (Vacuole) were separated by SDS-PAGE and transferred to nitrocellulose membrane. The β -gal lane contains purified β -galactosidase. Vacuoles were purified as previously described (Cardenas and Heitman 1995). The membrane was probed with antibodies against bacterial β -gal protein, as well as the yeast proteins CPY, Kar2, and Pma1.

flotation on a Ficoll gradient (Cardenas and Heitman 1995), and analyzed for presence of the Cos16-LacZ fusion protein. The intact Cos16-LacZ fusion was enriched in the vacuolar extract to an extent that was comparable to the vacuolar luminal marker, CPY (Figure 5). By contrast, the ER protein, Kar2, and the plasma-membrane protein, Pma1, were not significantly enriched in the vacuolar fraction (Figure 5). Similar studies using vacuolar vesicles purified by a different method (Ohsumi and Anraku 1981) yielded identical results (data not shown). These results suggest that Cos16 is an integral membrane protein of the vacuole.

Misfolded membrane proteins default to the vacuole (Stack and Emr 1993). However, that seems an unlikely explanation for the vacuolar localization of the Cos16-LacZ fusion protein, because single-copy *COS16-lacZ* complemented all of the *cos16* Δ phenotypes (data not shown). Moreover, a different epitope-tagged *COS16* fusion, in which the myc epitope was fused to the C terminus of Cos16, was functional, and exhibited a similar localization pattern (data not shown). Thus, the vac-

uolar localization of the Cos16-LacZ fusion protein probably reflects the subcellular location of the native Cos16 protein.

Cos16 and Mn²⁺ homeostasis: Because the vacuole sequesters Mn²⁺ from the cytosol (Okorokov *et al.* 1977), we examined if Cos16 was also involved in Mn²⁺ homeostasis. The *cos16* Δ ::*HIS3* deletion had a modest effect, similar to that of the *vps4* mutation, on the Mn²⁺ sensitivity of an otherwise wild-type strain (data not shown). Mutations in the Golgi Mn²⁺ transporter gene, *PMR1*, increase sensitivity to Mn²⁺ as the result of Mn²⁺ accumulation in the cytosol (Lapinskas *et al.* 1995). The *cos16* Δ ::*HIS3* deletion exacerbated this sensitivity (Figure 6A). Thus, deletion of *COS16* altered tolerance to Mn²⁺.

We also examined the effect of *COS16* on the chelator sensitivities of several Mn²⁺-homeostasis mutants. Strains lacking Pmr1 function are sensitive to EGTA, and this sensitivity can be ameliorated by increasing Mn²⁺ influx across the plasma membrane (Paidhungat and Garrett 1998). As shown in Figure 6B, the *cos16* Δ ::*HIS3* deletion allowed a *pmr1* Δ ::*LEU2* strain to grow on medium containing 0.5 mM EGTA. Mutations in *SMF1* also cause cells to become sensitive to EGTA, in this case as the result of the loss of a high-affinity Mn²⁺ uptake system. This EGTA sensitivity is alleviated by Mn²⁺ supplement (Supek *et al.* 1996), as well as overproduction of Cdc1 (Paidhungat and Garrett 1998). Again, only the *cos16* Δ ::*HIS3 smf1* Δ ::*URA3* double mutant tolerated 4 mM EGTA in the medium (Figure 6C). Finally, the EGTA sensitivity (1.5 mM) of the *cdc1-1*(Ts) strain was alleviated by the *cos16* Δ ::*HIS3* deletion (Figure 6D). These findings implicate Cos16 in Mn²⁺ homeostasis and suggest Cos16 is involved in the sequestration of Mn²⁺ into the vacuole. The last result is also consistent with the notion that the *cos16* mutations alleviate the *cdc1*(Ts) conditional growth defect through their effect on Mn²⁺ homeostasis.

Mn²⁺ content of *cdc1* and *cos16* mutants: Several genes that affect Mn²⁺ homeostasis, including *PMR1* and *ATX2*, alter intracellular Mn²⁺ content (Lapinskas *et al.* 1995; Lin and Culotta 1996). By contrast, intracellular Mn²⁺ levels are unaffected by overexpression of *CCC1*, a high-copy suppressor of the *pmr1* Mn²⁺ defect (Lapinskas *et al.* 1996). Because our results suggested that Cdc1 and Cos16 affected the intracellular distribution of Mn²⁺, we examined if mutations in either *CDC1* or *COS16* altered intracellular Mn²⁺ levels as judged by atomic absorption spectroscopy. The Mn²⁺ content of *cdc1-1*(Ts) (38.9 ± 8.3 pmols/A₆₀₀) and *cos16* Δ ::*HIS3* (41.4 ± 12.3 pmols/A₆₀₀) mutants were similar to the Mn²⁺ content of the isogenic wild-type (41.2 ± 7.0 pmols/A₆₀₀) strain, suggesting that depletion of neither Cdc1 nor Cos16 had a significant effect on whole-cell Mn²⁺ content. Cellular Mn²⁺ levels were also unaffected by *CDC1* overexpression (data not shown). Thus, both Cdc1 and Cos16 seem to affect the intracellular distribution of Mn²⁺ without changing the overall cellular content.

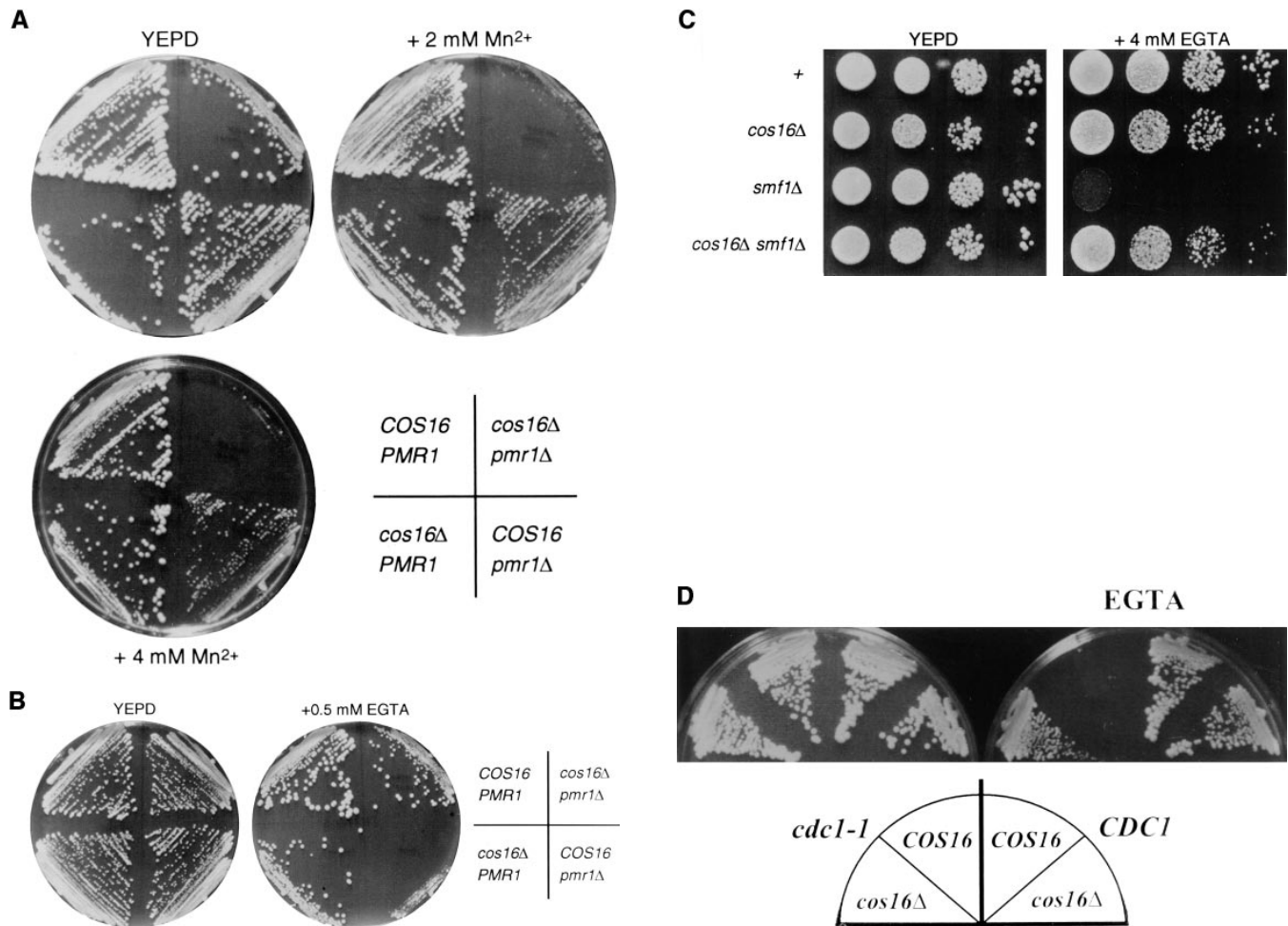


Figure 6.—*COS16* and Mn²⁺ homeostasis. (A) *cos16Δ* exacerbates the Mn²⁺ sensitivity of a *pmr1Δ* mutant. The indicated strains were streaked onto YEPD pH 5.5 agar, supplemented with 0 mm, 2 mm, or 4 mm MnCl₂, and incubated at 30° for 3–5 days. Strains were: *cos16Δ pmr1Δ* (FY70 *cos16Δ::HIS3 pmr1Δ::LEU2*); *COS16 pmr1Δ* (FY70 *pmr1Δ::HIS3*), *cos16Δ PMR1* (FY70 *cos16Δ::HIS3*); *COS16 PMR1* (FY70). (B) *cos16Δ* suppresses the EGTA sensitivity of a *pmr1Δ* mutant. The strains of panel A were streaked onto YEPD agar, supplemented with 0 mm or 0.5 mm EGTA, and incubated at 30° for 3–5 days. (C) *cos16Δ* suppresses the EGTA sensitivity of a *smf1Δ* mutant. 10-fold dilutions of exponentially growing cultures of the indicated strains were spotted onto YEPD agar or YEPD agar containing 4 mm EGTA, and incubated at 30° for 3 days. Strains were: + (FY70), *cos16Δ* (FY70 *cos16Δ::HIS3*), *smf1Δ* (FY70 *smf1Δ::URA3*), and *cos16Δ smf1Δ* (FY70 *cos16Δ::HIS3 smf1Δ::URA3*). (D) *cos16Δ* suppresses the EGTA sensitivity of a *cdc1-1(Ts)* mutant. The indicated strains were streaked onto YEPD agar or YEPD agar containing 1.5 mm EGTA and incubated at 30° for 3 days. Strains were: *cdc1 cos16Δ* (FY11 *cos16Δ::HIS3*); *cdc1* (FY11); *CDC1* (FY70); *cos16Δ* (FY70 *cos16Δ::HIS3*).

Cdc1 is dispensable in *cos16Δ* mutants: Because *Cos16* seemed to be involved in vacuolar Mn²⁺ homeostasis, we determined if a *cdc1Δ cos16Δ* double mutant could grow in the presence of exogenous Mn²⁺. Isogenic diploids (*cdc1Δ::HIS3/CDC1 COS16/COS16* and *cdc1Δ::HIS3/CDC1 cos16Δ::LEU2/COS16*) were sporulated and dissected onto YEPD medium agar with, or without, Mn²⁺ supplement. Two viable His⁻ (*CDC1*⁺) segregants were recovered from each tetrad of the *cdc1Δ::HIS3/CDC1 COS16/COS16* diploid (Figure 7), and the 2:0 segregation was not affected by Mn²⁺ (data not shown). By contrast, tetrads from the *cdc1Δ::HIS3/CDC1 cos16Δ::LEU2/COS16* diploid yielded 60% of the expected *cdc1Δ::HIS3 cos16Δ::LEU2* segregants (Figure 7). Thus, *Cdc1* is not essential in strains lacking *Cos16* function. Moreover,

>90% of the expected *cdc1Δ::HIS3 cos16Δ::LEU2* progeny formed healthy colonies when supplemented with 2 mm or 4 mm Mn²⁺ (Figure 7). Thus, Mn²⁺ augments the ability of the *cos16Δ* deletion to bypass *Cdc1* function.

DISCUSSION

Previous studies implicated *Cdc1* in the regulation of intracellular Mn²⁺ (Loukin and Kung 1995; Paidhungat and Garrett 1998). That hypothesis was based on several observations, including: (1) Mn²⁺ supplement partially alleviated the conditional *cdc1(Ts)* growth defect; and (2) *CDC1* overexpression ameliorated the EGTA sensitivity of two, unrelated Mn²⁺-homeostasis mutants.

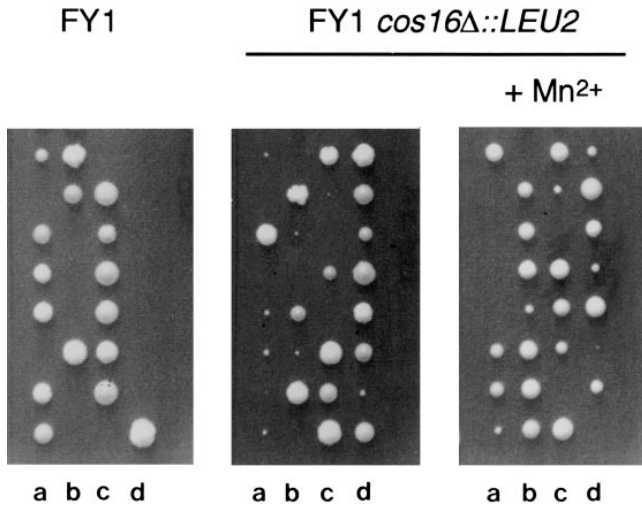


Figure 7.—Cdc1 is dispensable in a *cos16* mutant. Heterozygous *cdc1Δ::HIS3/CDC1 COS16/COS16* (FY1) or *cdc1Δ::HIS3/CDC1 cos16Δ::LEU2/COS16* (FY1 *cos16Δ::LEU2*) diploids were sporulated and dissected onto rich yeast medium with, or without, Mn^{2+} supplement (see materials and methods). Tiny (or small) colonies were *cdc1Δ::HIS3 cos16Δ::LEU2* as determined by their growth on minimal medium agar lacking histidine and leucine. (a, b, c, and d refer to individual spores of a tetrad.)

We show here that, in certain genetic backgrounds, Mn^{2+} supplement completely bypasses the essential Cdc1 requirement. Indeed, a *cdc1Δ cos16Δ* double mutant exhibits robust growth when the medium is supplemented with Mn^{2+} (Figure 7). Because *COS16* is also involved in intracellular Mn^{2+} homeostasis, these results are best explained by a model in which Mn^{2+} regulation is the single, essential function of Cdc1. These results also rule out the possibility that the Mn^{2+} dependence of *cdc1* strains reflects the fact that Cdc1 is a Mn^{2+} -dependent enzyme (Supek *et al.* 1996; Paidhungat and Garrett 1998).

Although the mechanism by which Cdc1 affects intracellular Mn^{2+} levels is not clear, the evidence favors a model in which Cdc1 functions to maintain cytosolic Mn^{2+} . Mn^{2+} depletion from the Golgi elicits a protein glycosylation defect not observed in the *cdc1*(Ts) mutants, and the *cdc1*(Ts) growth defect is exacerbated, not alleviated, by alterations that increase Mn^{2+} flux from the cytosol to the Golgi (Paidhungat and Garrett 1998). Thus, we suggested that the cytosol, rather than the Golgi apparatus, was the more likely site of *cdc1*(Ts) Mn^{2+} depletion (Paidhungat and Garrett 1998). Another major intracellular Mn^{2+} store is the vacuole (Okorokov *et al.* 1977). Although the vacuole is known to play a role in Mn^{2+} detoxification, nothing is known about the cellular function(s) of the vacuolar Mn^{2+} pool. However, mutations that inhibit vacuolar biogenesis (and function) at several distinct steps suppress, rather than exacerbate, the *cdc1*(Ts) growth defect. Suppression of conditional growth probably results

from the block in vacuolar Mn^{2+} sequestration because the same vacuolar biogenesis mutations also relieve the EGTA-sensitive phenotype of the *cdc1*(Ts) mutants (data not shown). These results eliminate the vacuole as the essential, Cdc1-dependent Mn^{2+} store and suggest that the vacuolar biogenesis mutations suppress the *cdc1*(Ts) growth defect by attenuating the depletion of cytosolic Mn^{2+} .

Lesions in vacuole biogenesis (*VPS*) genes affect many vacuolar functions, including proteolysis, Ca^{2+} accumulation, proton uptake and Mn^{2+} sequestration. However, the conditional *cdc1*(Ts) growth defect is suppressed only by mutations that affect the last of these processes. In particular, the *cdc1*(Ts) growth defect is suppressed by the inactivation of a protein, Cos16, that appears to be involved in Mn^{2+} sequestration into the vacuole. Several lines of evidence support this assertion. First, Cos16 is an integral membrane protein of the vacuole, as judged by the subcellular localization pattern of a functional Cos16-LacZ fusion protein (Figure 5). This observation is consistent with the presence of eight putative transmembrane domains within the predicted coding region. Thus, Cos16 is appropriately positioned to affect transport between the cytosol and vacuole. Second, a *cos16Δ* deletion suppresses the chelator sensitivity of a strain (*smf1Δ*) compromised for Mn^{2+} uptake into the cytosol (Figure 6C), suggesting that loss of Cos16 function compensates for the low influx into the cytosol. *cos16* mutations also relieve the chelator sensitivity of a mutant (*pnr1Δ*) that can be efficiently suppressed by genetic manipulations that raise cytosolic Mn^{2+} (Figure 6B; Paidhungat and Garrett 1998). Finally, Cos16 inactivation exacerbates the Mn^{2+} sensitivity of both wild-type (data not shown) and *pnr1Δ* mutant strains (Figure 6A), presumably by aggravating the accumulation of cytosolic Mn^{2+} . Thus, Cos16 appears to antagonize the *cdc1*(Ts) growth defect by sequestering cytosolic Mn^{2+} into the vacuole.

If *COS16* and *CDC1* are involved in the homeostasis of intracellular Mn^{2+} , why do intracellular Mn^{2+} levels not vary with changes in Cos16 or Cdc1 function? A previous report (Okorokov *et al.* 1977) suggested that most intracellular Mn^{2+} is found in the vacuole. According to that report, a defect in cytosolic Mn^{2+} retention, as predicted for *cdc1*(Ts) mutants, might not affect total intracellular Mn^{2+} content. However, it is harder to reconcile the fact that the *cos16Δ* deletion did not alter the level of intracellular Mn^{2+} . We can think of several possible explanations for this apparent paradox. First, Cos16 might either be involved in the regulation of other ions, or affect an organelle that might copurify with the vacuole. Although we have not formally ruled out these possibilities, they do not easily account for the observation that *cos16* mutations affect the growth of Mn^{2+} homeostasis mutants. Alternatively, Cos16 inactivation might block cytosolic to vacuole Mn^{2+} transfer without having a measurable effect on vacuolar Mn^{2+} content.

Finally, along with *COS16* and the vacuolar biogenesis genes characterized in this study, we identified several other suppressors of the *cdc1(Ts)* growth defect. One suppressor, *cos13*, falls within the same phenotypic and epistasis group as *cos16* and might, therefore, identify a component of a complex or pathway involved in vacuolar Mn²⁺ homeostasis. By contrast, the remaining recessive suppressors (*cos1*, *cos3*, *cos14*, *cos2*, *cos7*, and *cos10*) confer phenotypes that are not obviously related to Mn²⁺ regulation. Thus, the genes corresponding to these suppressors might specify receptors of the Cdc1 (and Mn²⁺)-dependent growth process. Future studies of these genes might help elucidate the role of Cdc1 in Mn²⁺ homeostasis and growth.

We thank M. Cardenas, V. Culotta, L. Davis, K. Dolinsky, J. Heitman, M. Hiller, E. W. Jones, R. Kahn and M. D. Rose for yeast strains, plasmids and antisera. M.P. also thanks T. Graf and J. Johnson for help and instruction with atomic absorption spectroscopy.

LITERATURE CITED

- Banta, L. M., J. S. Robinson, D. J. Klionsky and S. D. Emr, 1988 Organelle assembly in yeast: characterization of yeast mutants defective in vacuolar biogenesis and protein sorting. *J. Cell Biol.* **107**: 1369–1383.
- Banta, L. M., T. A. Vida, P. K. Herman and S. D. Emr, 1990 Characterization of yeast Vps33p, a protein required for vacuolar protein sorting and vacuole biogenesis. *Mol. Cell Biol.* **10**: 4638–4649.
- Cardenas, M. E., and J. Heitman, 1995 FKBP12-rapamycin target *TOR2* is a vacuolar protein with an associated phosphatidylinositol-4 kinase activity. *EMBO J.* **14**: 5892–5907.
- Casadaban, M. J., A. Martinez-Arias, S. K. Shapiro and J. Chou, 1983 β -Galactosidase gene fusions for analyzing gene expression in *Escherichia coli* and yeast. *Methods Enzymol.* **100**: 293–308.
- Cowles, C. R., S. D. Emr and B. F. Horazdovsky, 1994 Mutations in the *VPS45* gene, a *SECI* homologue, result in vacuolar protein sorting defects and accumulation of membrane vesicles. *J. Cell Sci.* **107**: 3449–3459.
- Eide, D., and M. L. Guerinot, 1997 Metal ion uptake in eukaryotes. *ASM News* **63**: 199–205.
- Garrett, S., and J. Broach, 1989 Loss of Ras activity in *Saccharomyces cerevisiae* is suppressed by disruption of a new kinase gene, *YAK1*, whose product may act downstream of the cAMP-dependent protein kinase. *Genes Dev.* **3**: 1336–1348.
- Hartwell, L., J. Culotti and B. J. Reid, 1970 Genetic control of the cell division cycle in yeast. I. Detection of mutants. *Proc. Natl. Acad. Sci. USA* **66**: 352–359.
- Horazdovsky, B. F., and S. D. Emr, 1993 The *VPS16* gene product associates with a sedimentable protein complex and is essential for vacuolar proteins sorting in yeast. *J. Biol. Chem.* **268**: 4953–4962.
- Iida, H., S. Sakaguchi, Y. Yagawa and Y. Anraku, 1990 Cell cycle control by Ca²⁺ in *Saccharomyces cerevisiae*. *J. Biol. Chem.* **265**: 21216–21222.
- Jones, E. W., G. S. Zubenko and R. R. Parker, 1982 *PEP4* gene function is required for expression of several vacuolar hydrolases in *Saccharomyces cerevisiae*. *Genetics* **102**: 665–677.
- Kyte, J., and R. F. Doolittle, 1982 A simple method for displaying the hydropathic character of a protein. *J. Mol. Biol.* **157**: 105–132.
- Lapinskas, P. J., K. W. Cunningham, X. F. Liu, G. R. Fink and V. C. Culotta, 1995 Mutations in *PMR1* suppress oxidative damage in yeast cells lacking superoxide dismutase. *Mol. Cell Biol.* **15**: 1382–1388.
- Lapinskas, P. J., S. Lin and V. C. Culotta, 1996 The role of the *Saccharomyces cerevisiae CCC1* gene in the homeostasis of manganese ions. *Mol. Microbiol.* **21**: 519–528.
- Lin, S.-J., and V. C. Culotta, 1996 Suppression of oxidative damage by *Saccharomyces cerevisiae ATX2*, which encodes a manganese-transporting protein that localizes to Golgi-like vesicles. *Mol. Cell Biol.* **16**: 6303–6312.
- Loukin, S., and C. Kung, 1995 Manganese effectively supports yeast cell-cycle progression in place of calcium. *J. Cell Biol.* **131**: 1025–1037.
- Manolson, M. F., D. Proteau, R. A. Preston, A. Stenbit, B. T. Roberts *et al.*, 1992 The *VPH1* gene encodes a 95-kDa integral membrane polypeptide required for *in vivo* assembly and activity of the yeast vacuolar H⁺-ATPase. *J. Biol. Chem.* **267**: 14294–14303.
- Munn, A. L., and H. Riezman, 1994 Endocytosis is required for the growth of vacuolar H⁺-ATPase-defective yeast: identification of six new *END* genes. *J. Cell Biol.* **127**: 373–386.
- Myers, A. M., A. Tzagoloff, D. M. Kinney and C. J. Lusty, 1986 Yeast shuttle and integrative vectors with multiple cloning sites suitable for construction of *lacZ* fusions. *Gene* **45**: 299–310.
- Nagasu, T., Y.-I. Shimma, Y. Nakanishi, J. Kuromitsu, K. Iwama *et al.*, 1992 Isolation of new temperature-sensitive mutants of *Saccharomyces cerevisiae* deficient in mannose outer chain elongation. *Yeast* **8**: 535–547.
- Ohsumi, Y., and Y. Anraku, 1981 Active transport of basic amino acids driven by a proton motive force in vacuolar membrane vesicles of *Saccharomyces cerevisiae*. *J. Biol. Chem.* **256**: 2079–2082.
- Okorokov, L. A., L. P. Lichko, V. M. Kadomtseva, V. P. Kholodenko, V. T. Titovsky *et al.*, 1977 Energy-dependent transport of manganese into yeast cells and distribution of accumulated ions. *Eur. J. Biochem.* **75**: 373–377.
- Paidhungat, M., and S. Garrett, 1998 Cdc1 is required for growth and Mn²⁺ regulation in *Saccharomyces cerevisiae*. *Genetics* **148**: 1777–1786.
- Preston, R. A., P. S. Reinagel and E. W. Jones, 1992 Genes required for vacuolar acidity in *Saccharomyces cerevisiae*. *Genetics* **131**: 551–558.
- Preston, R. A., M. F. Manolson, K. Becherer, E. Weidenhammer, D. Kirkpatrick *et al.*, 1991 Isolation and characterization of *PEP3*, a gene required for vacuolar biogenesis in *Saccharomyces cerevisiae*. *Mol. Cell Biol.* **11**: 5801–5812.
- Raymond, C. K., I. Howald-Stevenson, C. A. Vater and T. H. Stevens, 1992 Morphological classification of the yeast vacuolar protein sorting mutants: evidence for a prevacuolar compartment in class E *vps* mutants. *Mol. Biol. Cell* **3**: 1389–1402.
- Riles, L., J. E. Dutchik, A. Baktha, B. K. McCauley, E. C. Thayer *et al.*, 1993 Physical maps of the six smallest chromosomes of *Saccharomyces cerevisiae* at a resolution of 2.6 kilobase pairs. *Genetics* **134**: 81–150.
- Roberts, C. J., C. K. Raymond, C. T. Yamashiro and T. H. Stevens, 1991 Methods for studying the yeast vacuole, in *Guide to Yeast Genetics and Molecular Biology*. Academic Press, San Diego.
- Robinson, J. S., T. R. Graham and S. D. Emr, 1991 A putative zinc finger protein, *Saccharomyces cerevisiae* Vps18p, affects late Golgi functions required for vacuolar protein sorting and efficient α -factor prohormone maturation. *Mol. Cell Biol.* **12**: 5813–5824.
- Rose, M. D., P. Novick, J. H. Thomas, D. Botstein and G. Fink, 1987 A *Saccharomyces cerevisiae* genomic plasmid bank based on a centromere-containing shuttle vector. *Gene* **60**: 237–243.
- Sikorski, R. S., and P. Hieter, 1989 A system of shuttle vectors and yeast host strains designed for efficient manipulation of DNA in *Saccharomyces cerevisiae*. *Genetics* **122**: 19–27.
- Stack, J. H., and S. D. Emr, 1993 Genetic and biochemical studies of protein sorting to the yeast vacuole. *Curr. Opin. Cell Biol.* **5**: 641–646.
- Stearns, T., M. C. Willingham, D. Botstein and R. A. Kahn, 1990 ADP-ribosylation factor is functionally and physically associated with the Golgi complex. *Proc. Natl. Acad. Sci. USA* **87**: 1238–1242.
- Supek, F., L. Supekova, H. Nelson and N. Nelson, 1996 A yeast manganese transporter related to the macrophage protein involved in conferring resistance to mycobacteria. *Proc. Natl. Acad. Sci. USA* **93**: 5105–5110.
- Wedler, F. C., 1994 Biochemical and nutritional role of manganese: an overview, pp. 1–38 in *Manganese in Health and Disease*, edited by D. J. Klimis-Tavantzis. CRC Press, Inc., Boca Raton, FL.
- Weisman, L. S., and W. Wickner, 1992 Molecular characterization of *VAC1*, a gene required for vacuole inheritance and vacuole protein sorting. *J. Biol. Chem.* **267**: 618–623.
- Woodcock, D. M., P. J. Crowther, J. Doherty, S. Jefferson, E. Decruz *et al.*, 1989 Quantitative evaluation of *Escherichia coli*

- host strains for tolerance to cytosine methylation in plasmid and phage recombinants. *Nucleic Acids Res.* **17**: 3469–3478.
- Woolford, C. A., C. K. Dixon, M. F. Manolson, R. Wright and E. W. Jones, 1990 Isolation and characterization of *PEP5*, a gene essential for vacuolar biogenesis in *Saccharomyces cerevisiae*. *Genetics* **125**: 739–752.
- Youatt, J., and I. McKinnon, 1993 Manganese (Mn^{2+}) reverses the inhibition of fungal growth by EGTA. *Microbios* **74**: 181–196.

Communicating editor: M. Johnston